

Supplementary Material for

“Regional modelling of polycyclic aromatic hydrocarbons: WRF/Chem-PAH model development and East Asia case studies”

Qing Mu, Gerhard Lammel, Christian N. Gencarelli, Ian M. Hedgecock, Ying Chen, Petra Příbylová, Monique Teich, Yuxuan Zhang, Guangjie Zheng, Dominik van Pinxteren, Qiang Zhang, Hartmut Herrmann, Manabu Shiraiwa, Peter Spichtinger, Hang Su, Ulrich Pöschl, Yafang Cheng

Table of Contents

Table S1. Configurations of WRF/Chem v3.6.1

Table S2. Parameterization of heterogeneous reaction rate for the ozonolysis of BaP.

Figure S1. Air-soil gas exchange flux and near-ground air concentration.

Figure S2. Emissions of PAHs in July 2013.

Figure S3. Simulated and observed concentrations of gaseous and particulate PAHs at the Xianghe site during 11–22 July, 2013.

Figure S4. Simulated and observed daily, day and night average concentrations of BC, OC and particulate mass fraction of CHR at the Xianghe site. Calculated particulate mass fraction of CHR based on observed BC and OC is also shown.

Figure S5. Simulated and observed concentrations of gaseous and particulate PAHs at the Gosan site during 14–25 February, 2003.

Figure S6. Simulated and observed concentrations of gas phase PHE and CHR, particulate phase BaP and CHR, and particulate mass fraction of CHR at the Gosan site averaged over 6–17 June 2003 (summer case). Error bars show the standard deviations.

Text S1. Overview of the heterogeneous degradation of BaP

Text S2. Sampling at the Xianghe site and data quality control

Table S3. Field blank concentrations (G: gas phase; P: particulate phase) and number of samples >LOQ out of total samples.

Table S1. Configurations of WRF/Chem v3.6.1

Physics	WRF option
Microphysics	Lin scheme
Surface layer	Eta Monin–Obukhov (Janjic) scheme
Planetary boundary layer	Mellor–Yamada–Janjic (MJY) TKE scheme
Cumulus parameterisation	Grell 3-D ensemble scheme
Land-surface model	Unified Noah land-surface model
Shortwave radiation	Goddard scheme
Longwave radiation	RRTMG scheme
Chemistry	Chem option
Gas-phase mechanism	RACM with aqua-phase reactions
Aerosol module	MADE/SORGAM
Photolytic rate	Fast-J photolysis scheme

Table S2. Parameterization of heterogeneous reaction rate for the ozonolysis of BaP. First-order reaction rate coefficients k (s^{-1}) are given by the Hill equation $k = \text{base} + \frac{\text{max}-\text{base}}{1+(\frac{\text{xhalf}}{[\text{O}_3]})^{\text{rate}}}$ with $[\text{O}_3]$

in ppbv. For each grid cell, the parameters are read from the look-up table with temperature and relative humidity (RH) closest to the temperature and humidity of the grid cell. When equally close, the smaller parameter value is adopted.

70% RH				
Temperature (°C)	base	max	rate	xhalf
40	1.67e-4	1.29e-2	0.682	1.25e3
35	1.19e-4	1.29e-2	0.682	1.25e3
30	8.52e-5	9.02e-3	0.696	1.23e3
25	5.94e-5	6.33e-3	0.707	1.27e3
23	4.84e-5	5.14e-3	0.700	1.25e3
15	2.55e-5	2.72e-3	0.711	1.29e3
10	1.58e-5	1.68e-3	0.706	1.27e3
5	9.49e-6	1.00e-3	0.698	1.24e3
0	6.85e-6	5.64e-4	0.704	1.11e3
-5	5.31e-6	3.10e-4	0.713	1.01e3
-10	3.83e-6	1.48e-4	0.731	7.33e2
-15	8.93e-7	1.05e-4	0.580	1.88e3
-20	1.16e-6	2.58e-5	0.673	3.35e2

50% RH				
Temperature (°C)	base	max	rate	xhalf
40	1.65e-4	1.80e-2	0.672	1.21e3
35	1.16e-4	1.27e-2	0.678	1.24e3
30	8.24e-5	8.68e-3	0.688	1.22e3
25	5.44e-5	5.71e-3	0.688	1.21e3
23	2.64e-5	3.08e-3	0.618	7.97e2
15	2.20e-6	1.10e-3	0.544	5.83e2
10	7.84e-7	2.60e-4	0.559	7.50e1
5	-4.79e-7	7.19e-5	0.564	1.31e1
0	-7.02e-6	2.18e-5	0.464	1.05e0
-5	-4.06e-6	6.54e-6	0.459	1.24e-1
-10	-1.89e-6	2.02e-6	0.429	1.44e-2
-15	2.58e-7	7.22e-7	0.175	1.28e-1
-20	1.79e-7	2.60e-7	0.689	1.11e3

Dry				
Temperature (°C)	base	max	rate	xhalf
40	1.61e-4	1.74e-2	0.667	1.19e3
35	1.10e-4	1.19e-2	0.667	1.21e3
30	6.75e-5	7.31e-3	0.653	1.11e3
25	2.3e-5	3.10e-3	0.586	7.02e2
23	-1.90e-5	9.28e-4	0.446	1.59e2
15	-2.65e-5	3.09e-4	0.341	8.38e1
10	-4.28e-5	1.03e-4	0.191	4.41e0
5	-1.12e-5	3.49e-5	0.142	4.33e0
0	3.39e-6	1.03e-5	0.382	8.85e2
-5	1.37e-6	5.67e-6	0.780	2.96e3

-10	4.53e-7	1.57e-6	0.979	1.63e3
-15	1.44e-7	2.10e-6	0.924	1.39e4

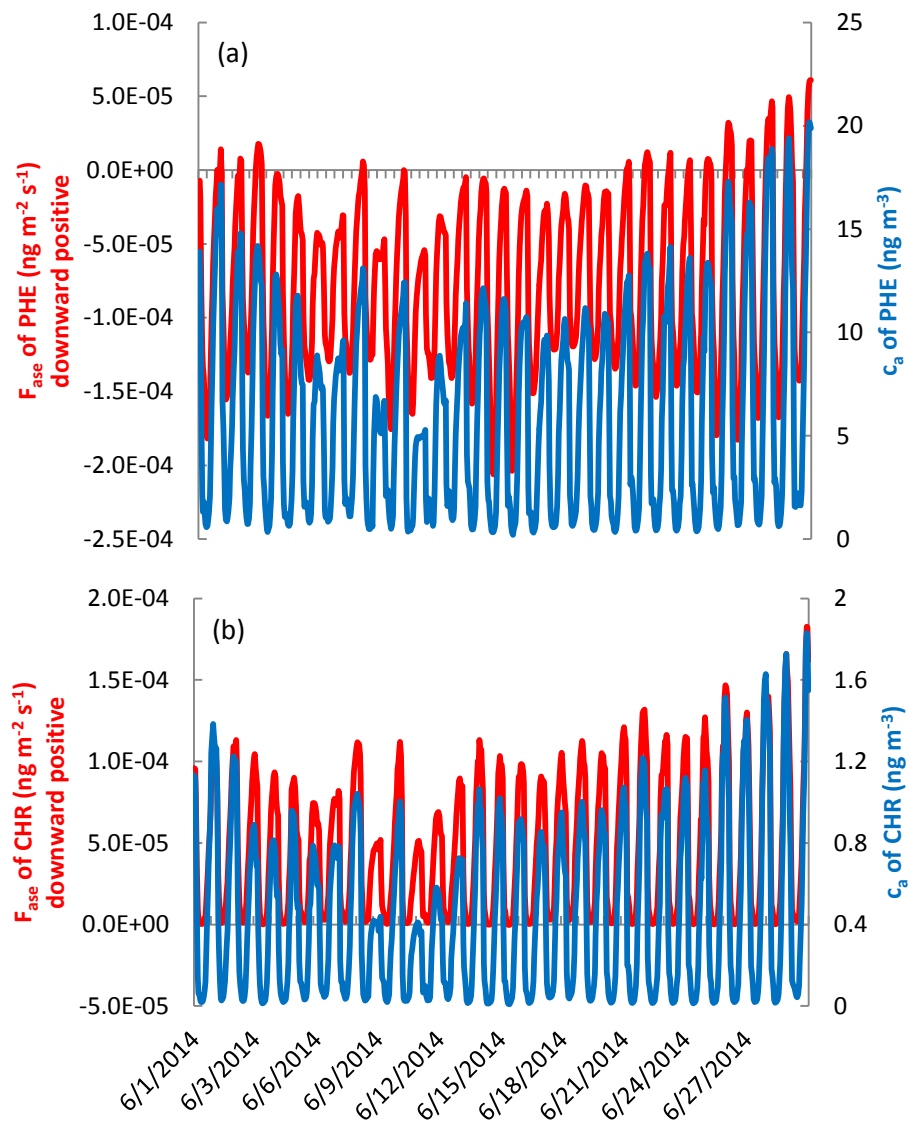


Figure S1. Air-soil gas exchange flux (F_{ase} , positive is defined downward, negative is defined upward) and near-ground air concentration (c_a) at a receptor site.

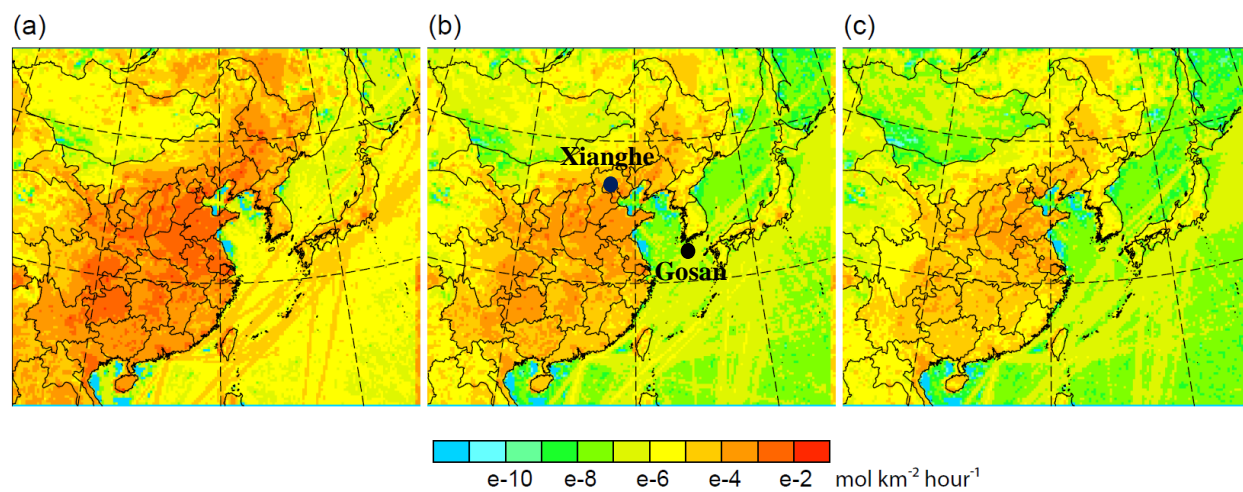


Figure S2. Emissions of (a) PHE, (b) CHR and (c) BaP in July 2013. The locations of Xianghe and Gosan are also shown.

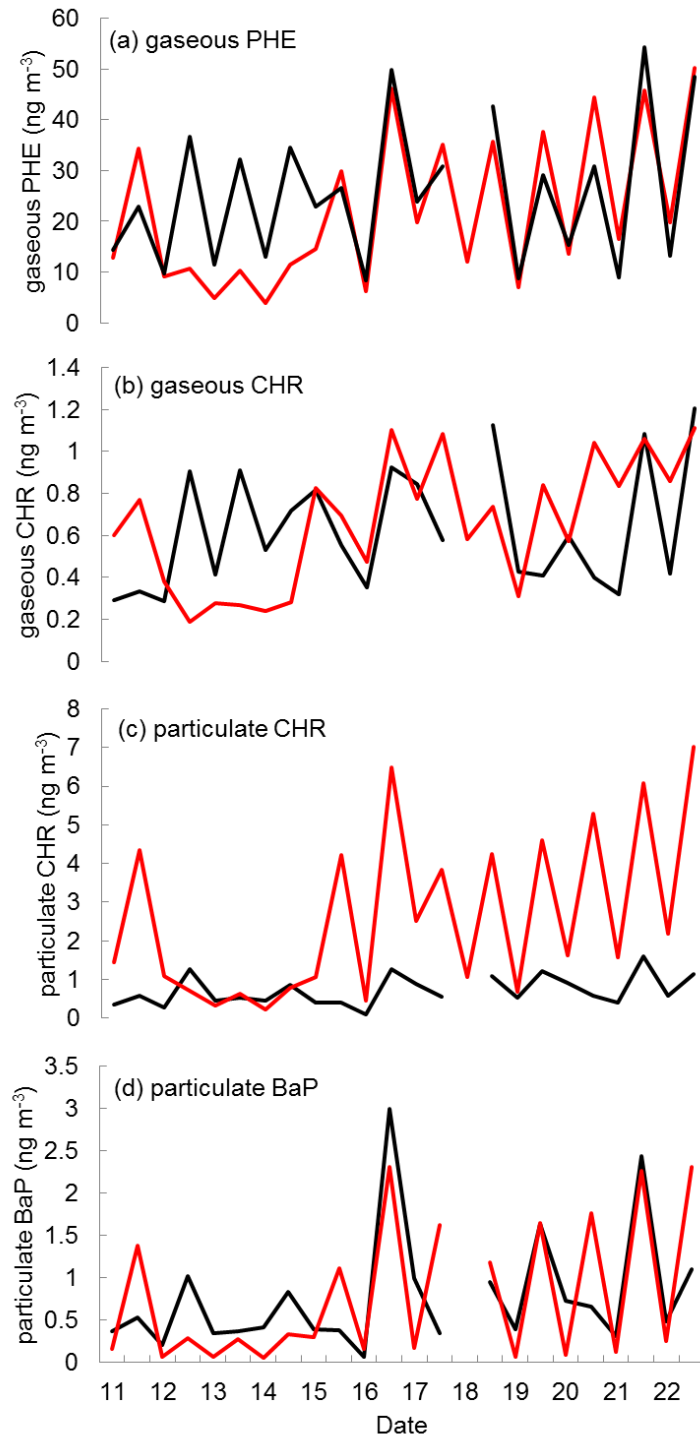


Figure S3. Simulated (red) and observed (black) concentrations of (a) gaseous PHE, (b) gaseous CHR, (c) particulate CHR and (d) particulate BaP at the Xianghe site during 11–22 July, 2013.

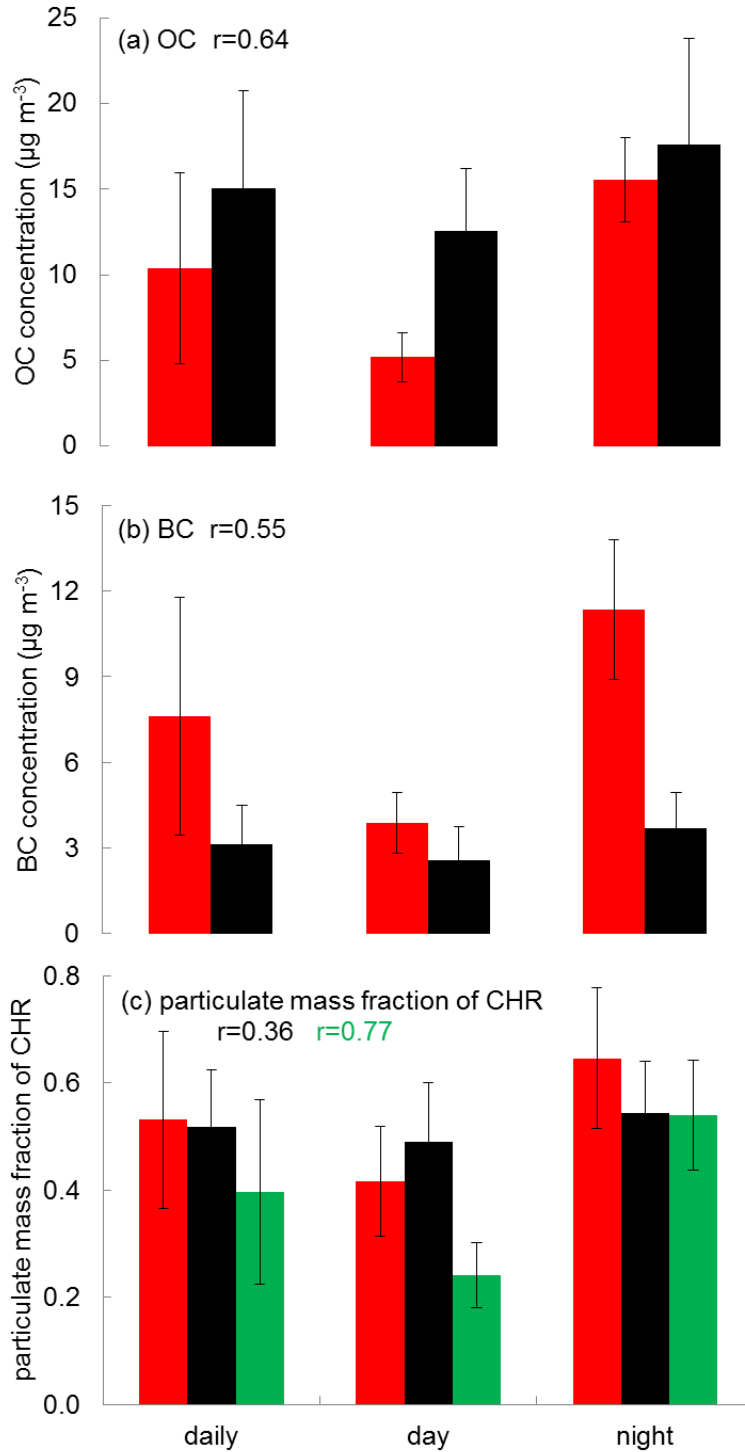


Figure S4. Simulated (red) and observed (black) daily, day and night average concentrations of (a) OC, (b) BC and (c) particulate mass fraction of CHR at the Xianghe site during 11–22 July, 2013. Calculated particulate mass fraction of CHR based on the observed BC and OC is shown in (c) green column. r is the correlation coefficient between observation and simulation. Error bar shows the standard deviations.

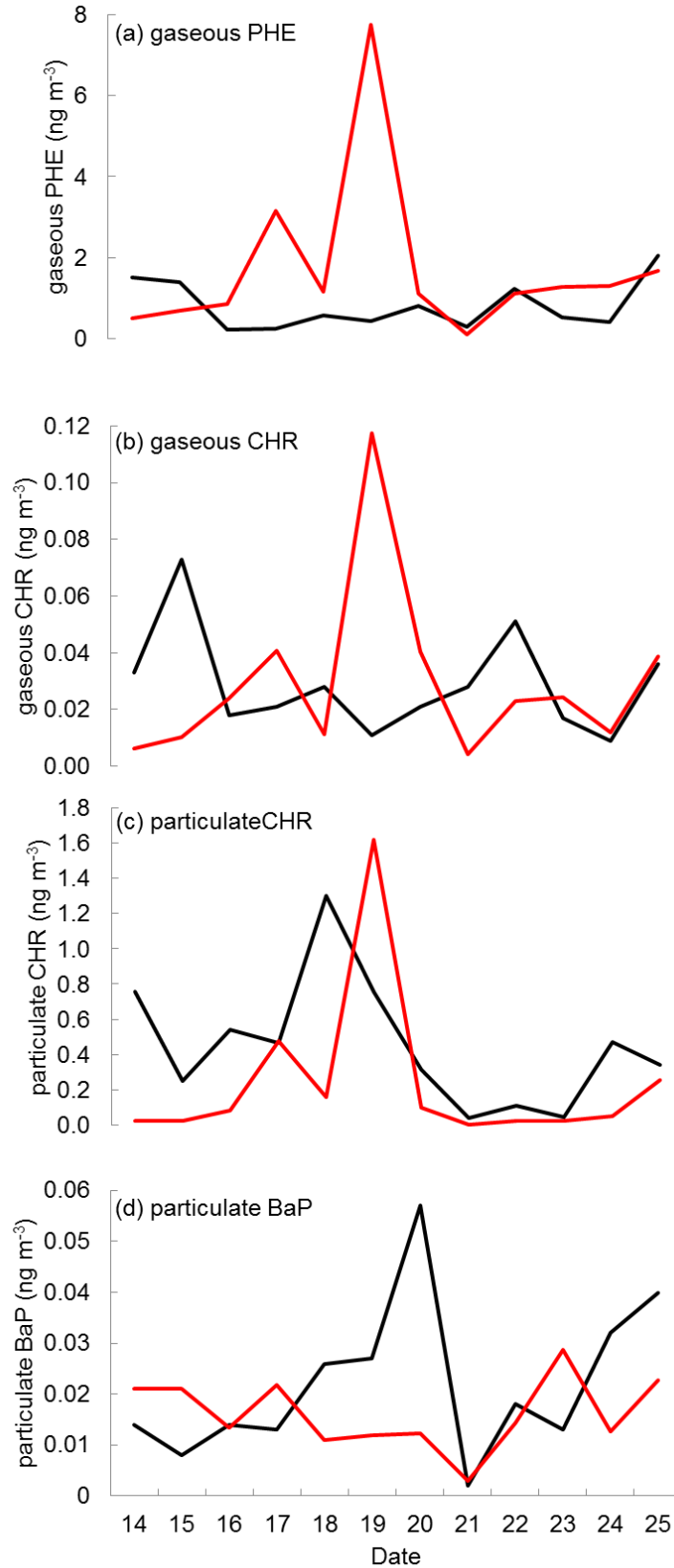


Figure S5. Simulated (red) and observed (black) concentrations of (a) gaseous PHE, (b) gaseous CHR, (c) particulate CHR and (d) particulate BaP at the Gosan site during 14–25 February, 2003.

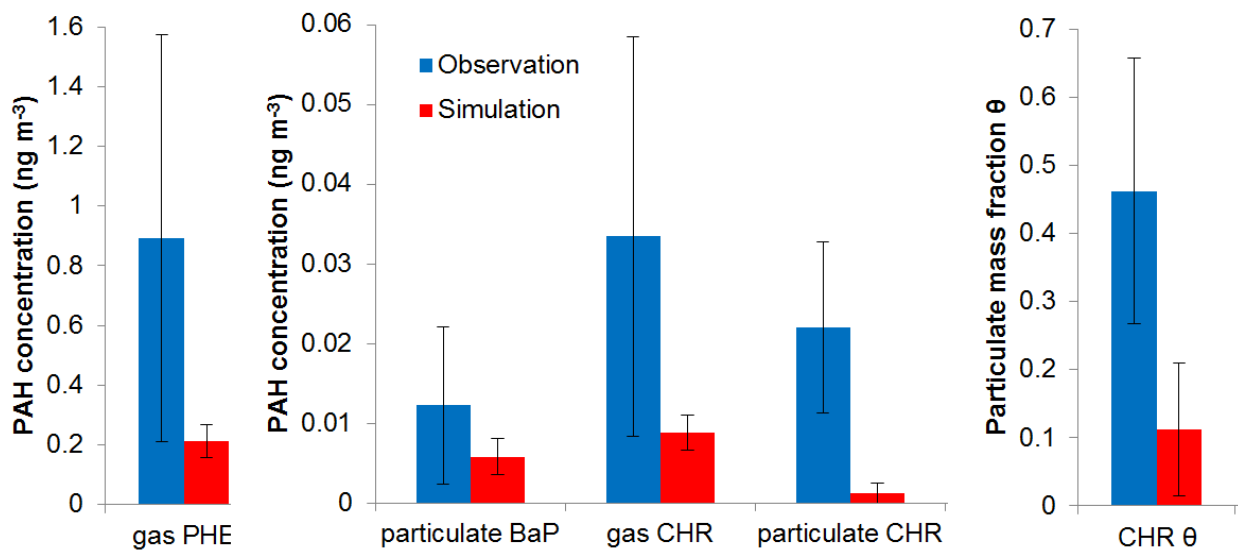


Figure S6. Simulated and observed concentrations of gas phase PHE and CHR, particulate phase BaP and CHR, and particulate mass fraction of CHR at the Gosan site averaged over 6–17 June 2003 (summer case). Error bars show the standard deviations.

Text S1. Overview of the heterogeneous degradation of BaP

In the atmosphere, BaP resides almost entirely in the particle phase of aerosols and undergoes heterogeneous reaction with ozone, but the reactivity is not well characterized for particles of complex composition and morphology. Laboratory experiments have shown that the reaction with ozone is fast on the surface of solid particles but decreases substantially on liquid substrates and in the presence of coatings that can shield BaP from the oxidant (Pöschl et al., 2001; Kwamena et al., 2004; Kahan et al., 2006; Shiraiwa et al., 2009; Zhou et al., 2012; Zhou et al., 2013). So far, however, laboratory data are available only at room temperature and some of the experiments were performed at unrealistically high ozone concentrations (up to 3 orders of magnitude above tropospheric levels). Field experiments indicate substantial but not very fast degradation of BaP on aerosols in ambient air (Schauer et al. 2003), and recent studies suggest that the phase state can strongly influence the rates of gas uptake, oxidation, and chemical aging of organic aerosol particles depending on temperature and relative humidity (e.g., Shiraiwa et al. 2011, Berkemeier et al. 2016). Following up on the laboratory experiments of Zhou et al. (2012) and Zhou et al. (2013), Shrivastava et al. (2017) applied a highly simplified parameterization to investigate the influence of temperature and humidity on the atmospheric degradation and transport of BaP and concluded that organic aerosol coatings can have a strong influence on lung cancer risks.

Text S1 References:

Berkemeier, T., Steimer, S. S., Krieger, U. K., Peter, T., Pöschl, U., Ammann, M., and Shiraiwa, M.: Ozone uptake on glassy, semi-solid and liquid organic matter and the role of reactive oxygen intermediates in atmospheric aerosol chemistry, *Phys. Chem. Chem. Phys.*, 18, 12662-12674, 10.1039/c6cp00634e, 2016.

Kahan, T. F., Kwamena, N. O. A., and Donaldson, D. J.: Heterogeneous ozonation kinetics of polycyclic aromatic hydrocarbons on organic films, *Atmos. Environ.*, 40, 3448-3459, 10.1016/j.atmosenv.2006.02.004, 2006.

Kwamena, N. O. A., Thornton, J. A., and Abbatt, J. P. D.: Kinetics of surface-bound benzo[a]pyrene and ozone on solid organic and salt aerosols, *J. Phys. Chem. A*, 108, 11626-11634, 10.1021/Jp046161x, 2004.

Pöschl, U., Letzel, T., Schauer, C., and Niessner, R.: Interaction of ozone and water vapor with spark discharge soot aerosol particles coated with benzo[a]pyrene: O₃ and H₂O adsorption, benzo[a]pyrene degradation, and atmospheric implications, *J. Phys. Chem. A*, 105, 4029-4041, 10.1021/Jp004137n, 2001.

Schauer, C., Niessner, R., and Pöschl, U.: Polycyclic aromatic hydrocarbons in urban air particulate matter: Decadal and seasonal trends, chemical degradation, and sampling artifacts, *Environ. Sci. Technol.*, 37, 2861-2868, 10.1021/es034059s, 2003.

Shiraiwa, M., Garland, R. M., and Pöschl, U.: Kinetic double-layer model of aerosol surface chemistry and gas-particle interactions (K2-SURF): Degradation of polycyclic aromatic hydrocarbons exposed to O₃, NO₂, H₂O, OH and NO₃, *Atmos. Chem. Phys.*, 9, 9571-9586, 10.5194/acp-9-9571-2009, 2009.

Shiraiwa, M., Ammann, M., Koop, T., and Pöschl, U.: Gas uptake and chemical aging of semisolid organic aerosol particles, *Proc. Natl. Acad. Sci. USA*, 108, 11003-11008, 10.1073/pnas.1103045108, 2011.

Shrivastava, M., Lou, S., Zelenyuk, A., Easter, R. C., Corley, R. A., Thrall, B. D., Rasch, P. J., Fast, J. D., Massey Simonich, S. L., Shen, H., and Tao, S.: Global long-range transport and lung cancer risk from polycyclic aromatic hydrocarbons shielded by coatings of organic aerosol, *Proceedings of the National Academy of Sciences*, 10.1073/pnas.1618475114, 2017.

Zhou, S., Lee, A. K. Y., McWhinney, R. D., and Abbatt, J. P. D.: Burial Effects of Organic Coatings on the Heterogeneous Reactivity of Particle-Borne Benzo[a]pyrene (BaP) toward Ozone, *J. Phys. Chem. A*, 116, 7050-7056, 10.1021/Jp3030705, 2012.

Zhou, S. M., Shiraiwa, M., McWhinney, R. D., Poschl, U., and Abbatt, J. P. D.: Kinetic limitations in gas-particle reactions arising from slow diffusion in secondary organic aerosol, *Faraday Discuss.*, 165, 391-406, 10.1039/C3fd00030c, 2013.

Text S2. Sampling at the Xianghe site and data quality control

Particulate- and gas-phase samples were collected twice a day (day time samples 8:00 – 18:00 LT, night time samples 20:00 – 6:00 LT) during 11–22 July 2013 using a low volume sampler at a flow rate of $2.3 \text{ m}^3 \text{ h}^{-1}$ (Leckel LVS, PM_{10} inlet) equipped with a quartz filter (Whatman QMA 47 mm) and 2 polyurethane foam (PUF) plugs (Gumotex Břeclav, density 0.030 g cm^{-3} , 55 mm diameter, total depth 10 cm, cleaned by extraction in acetone and dichloromethane, 8 h each, placed in a glass cartridge) in series. Field blanks were prepared (4 for particulate phase and 3 for gas-phase) following the standard protocol for mounting QFF and PUF plugs without turning on the sampler. PAHs were analyzed using gas-chromatography coupled to a mass spectrometer operated in the electron impact ionization mode. Breakthrough of the PUFs was not expected based on estimation of the safe sample volume (Kamprad and Goss, 2007; Melymuk et al., 2016), but nevertheless was controlled by separate analysis of PUF plugs in series and confirmed to not occur.

Limits of quantification (LOQ) were calculated based on instrument detection limits, which in turn are determined using 3 times the chromatogram baseline noise level: $\text{LOQ} = \text{mean blank concentrations} + 3 * \text{standard deviations (SD)}$. PAH concentrations are reported after subtraction of the mean field blank level (see Table S3). Only data points for which the concentrations exceeded the LOQ were considered. Therefore, gaseous PHE and CHR, and particulate phase CHR and BaP were used for the model evaluation, when all the samples with concentration exceeding LOQ. The field blank level of selected species corresponded to about 3-10% of the amounts collected in samples.

Table S3. Field blank concentrations (G: gas-phase; P: particulate phase; based on typical sampling volume) and percentage of samples with concentrations exceeding LOQ.

Species	Field blank concentrations (ng m^{-3})	Percentage of samples >LOQ
	Mean \pm SD	
PHE	G: 2.46 ± 0.57	100%
	P: 0.56 ± 0.06	34%
CHR	G: 0.07 ± 0.006	100%
	P: 0.03 ± 0.004	100%
BaP	G: 0.03	0
	P: < 0.03	100%

EC and OC samples were collected by a Digitel high volume air sampler DHA-80 (Riemer, Hausen, Germany) on quartz fiber filters (MK 360, Munktell, Falun, Sweden) at a flow rate of $0.5 \text{ m}^3 \text{ min}^{-1}$. For analyses of quartz filters the EUSAAR 2 temperature-protocol was used and a charring correction using light transmission was applied (Cavalli et al., 2010).

Text S2 References:

Cavalli, F., Viana, M., Yttri, K. E., Genberg, J., and Putaud, J. P.: Toward a standardised thermal-optical protocol for measuring atmospheric organic and elemental carbon: the EUSAAR protocol, *Atmos. Meas. Tech.*, 3, 79-89, 2010.

Melymuk, L., Bohlin-Nizzetto, P., Prokeš, R., Kukučka, P., and Klánová, J.: Sampling artifacts in active air sampling of semivolatile organic contaminants: Comparing theoretical and measured artifacts and evaluating implications for monitoring networks, *Environ. Pollut.*, 217, 97–106, 2016.

Kamprad, I. and Goss, K.: Systematic Investigation of the Sorption Properties of Polyurethane Foams for Organic Vapors, *Analytical Chemistry*, 79, 4222-4227, 2007.